

# Rheology and porosity effect on the proliferation of pre-osteoblast on zirconia ceramics

S Kulkov<sup>1,2</sup>, L Litvinova<sup>3</sup>, E Kalatur<sup>2</sup>, A Buyakov<sup>1,2</sup>

<sup>1</sup>Tomsk State University, 36, Lenin Avenue, Tomsk, 634050, Russia

<sup>2</sup>Institute of Strength Physics and Materials Science of Siberian Branch Russian Academy of Sciences 2/4, pr. Akademicheskii, Tomsk, 634021, Russia

<sup>3</sup>Immanuel Kant Baltic Federal University, Kaliningrad, Russia

e-mail: kulkov@ms.tsc.ru

**Abstract.** It has been studied  $ZrO_2(Me_xO_y)$  based porous ceramics, obtained from the powders consisting of hollow spherical particles. It was shown that the structure is represented as a cellular carcass with a bimodal porosity, formed of a large pore close to a spherical shape and the pores that were not filled with the powder particles during the compaction. For such ceramics the increase of pore volume is accompanied by an increase in strain in an elastic area. It was also shown that the porous  $ZrO_2$  ceramics had no acute or chronic cytotoxicity. At the same time, ceramics possess the osteoconductive properties: adhesion support, spreading, proliferation and osteogenic differentiation of MSCs.

## 1. Introduction

Porous ceramic materials have been successfully used in various fields, including as heat-insulating building materials, because they are durable, corrosion resistant and they possess stable thermal features [1-6]. Porous ceramics are also a promising material for medical use in the field of traumatology and orthopedics for critical sized bone defect recovery. Thus porous ceramics can act both as osteoplastic material or as 3D scaffold for tissue engineered bone equivalent modeling [7].

Ceramics based on partially stabilized zirconium are the most interesting among the variety of ceramic materials due to their inherent high fracture toughness because of their inherent transformational conversion. It is known that the characteristics are determined by the quality of source ceramic powder (particle shape, particle size distribution), the conditions of compacting and sintering modes and any features that are presented in each phase, and how these phases, including pores, are arranged in relation to each other. The most important factor in the successful application of materials is understanding the features of a structure emerging in them on their behavior under mechanical impact.

The aim of a paper is to examine the pore structure of  $ZrO_2(Me_xO_y)$  ceramics and its biocompatibility with multipotent mesenchymal stromal cells (MSCs) *in vitro* assays.

## 2. Materials and methods

The materials for the study were ceramics obtained from powders of  $ZrO_2(MgO)$ ,  $ZrO_2(Y_2O_3)$ , liquid-phase decomposition of precursors synthesized in high-frequency discharge plasma (the plasma chemistry method). Porous ceramic  $ZrO_2(MgO)$ ,  $ZrO_2(Y_2O_3)$  powder was prepared by pressing and subsequent sintering of compacts homologous temperatures ranging from 0.63 to 0.56 during the isothermal holding duration of 1 to 5 hours. The porosity of ceramics  $ZrO_2(MgO)$ ,  $ZrO_2(Y_2O_3)$  ranged



from 15 to  $\approx 45\%$  and  $\approx 30$  to  $80\%$ , respectively. X-ray studies were carried out on a diffractometer with filtered  $\text{CuK}\alpha$  radiation. The studies on the ceramic structure were carried out on the scanning electron microscope (SEM) Philips SEM 515.

To assess the biocompatibility of porous ceramics, the adipose-derived MSCs have been used. MSCs were isolated by enzymatic method and cultured in DMEM:F12 supplemented with 2 mM *L*-glutamine and 10% FBS ("Sigma", USA) and incubated with use of integrated continuous live cell imaging and analysis platform Cell IQ® v2 MLF ("CM Technologies"). Third passage MSCs have been used for experiments. Preliminarily MSC culture compliance with minimal criteria was made for phenotype (flow cytometry) and differentiation potential (differentiation assays for adipocytes and osteoblasts) [8]. Prior to seeding over the implants, cell viability in suspension was assessed by Trypan blue staining. [9] To assess the cytotoxicity of the implants and the viability of cultured MSCs over their surfaces, cell combined double staining with fluorescein diacetate (FDA) and propidium iodide (PI) 24h after inoculation and 7 days after culturing has been made [10]. Assessment of cytotoxicity was performed using an inverted fluorescent microscope Axio Observer A1 ("Carl Zeiss", Germany). To further biocompatibility assessment, the MSC osteogenic differentiation assay was performed according to standard protocols [11]. MSCs were cultured in implants or over its surface for 14 days, followed by detection of alkaline phosphatase activity using the BCIP/NBT substrate ("Sigma", USA) [12].

### 3. Results and discussion

#### 3.1. Powders

Figure 1. (a) represents the SEM-picture of  $\text{ZrO}_2$  powder (3 mol.%  $\text{Y}_2\text{O}_3$ ), synthesized by the method of plasma chemistry and particle size distribution of the powder size.  $\text{ZrO}_2$  powders (3 mol.%  $\text{MgO}$ ) and  $\text{ZrO}_2$ (3 mol.%  $\text{Y}_2\text{O}_3$ ) practically have no difference in morphological structure and they consist of hollow particles of a spherical shape and a large number of units having no regular form. The average particle size of the spherical powders  $\text{ZrO}_2(\text{MgO})$ ,  $\text{ZrO}_2(\text{Y}_2\text{O}_3)$  was 1.8 and 1.5 microns, respectively.

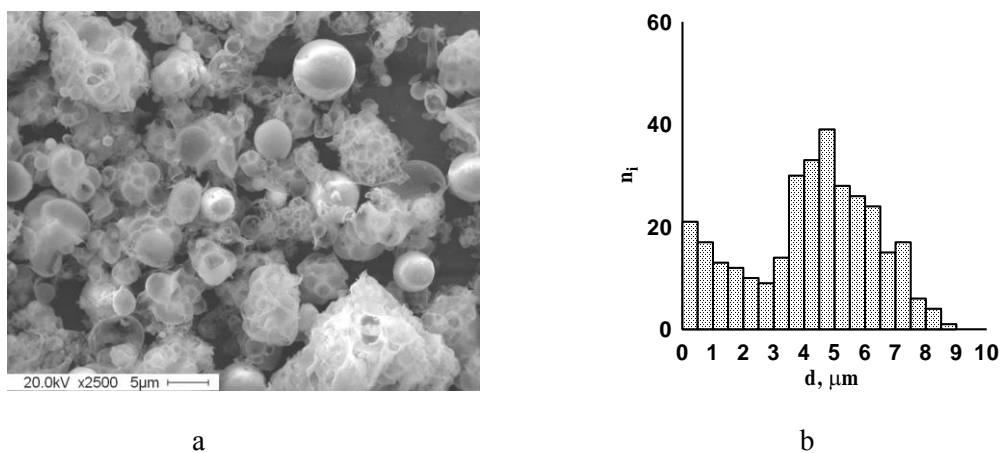


**Figure 1.** SEM - picture of  $\text{ZrO}_2$  powder ( $\text{Y}_2\text{O}_3$ ), synthesized by the method of plasma chemistry (a) and particle size distribution of  $\text{ZrO}_2$  powder ( $\text{Y}_2\text{O}_3$ ) size (b)

The phase composition of  $\text{ZrO}_2$  powder ( $\text{Y}_2\text{O}_3$ ) is presented by tetragonal and monoclinic  $\text{ZrO}_2$ . In the powder  $\text{ZrO}_2(\text{MgO})$  the cubic, tetragonal and monoclinic phases of  $\text{ZrO}_2$  were present. The rate of tetragonal  $\text{ZrO}_2$  powder  $\text{ZrO}_2(\text{Y}_2\text{O}_3)$  was about 95%, and  $\text{ZrO}_2$  in the cubic phase  $\text{ZrO}_2$  powder ( $\text{MgO}$ )

- 75%. The average size of the coherent scattering regions (SCR) tetragonal  $ZrO_2$  in  $ZrO_2$  powder ( $Y_2O_3$ ) was 20 nm, and the monoclinic modification - 50 nm. The average size of cubic modification SCR of  $ZrO_2$  in  $ZrO_2$  powder (MgO) was 20 nm, monoclinic  $ZrO_2$  - 30 nm, in the tetragonal phase - 15 nm.

### 3.2. Sintered ceramics

Figure 2 represents the SEM - picture of  $ZrO_2$  ceramics structure ( $Y_2O_3$ ) and pore size distribution.  $ZrO_2$  ceramics structure (MgO),  $ZrO_2(Y_2O_3)$  were represented as a cellular frame. Cells had a nearly spherical shape. The cell size exceeded by many times the thickness of the walls, which was represented as a single  $ZrO_2$  layer stacking grain.

Pore size distribution was bimodal. The first maximum pore was formed by interparticle pores that were not filled with powder particles during compaction and the second - with the larger pores close to a spherical shape. From the optical microscopy data we have obtained dependences of interparticles pores and larger spherical pores, it is seen that the increase in the volume of pores in the material from  $\approx 30$  to 80% was achieved by reducing the sintering temperature of the samples and it was accompanied by an increase in the average size of large pores from 2 to 6 microns. Changing the porosity of the material had practically no influence on the average size of interparticles pores, the average size of which was 0.5 microns. It can be assumed that the presence of large pores close to a spherical shape in the ceramics is due to the presence of hollow spherical particles in source powders, since their average size is commensurate with an average size of presented large pores in the sintered material.

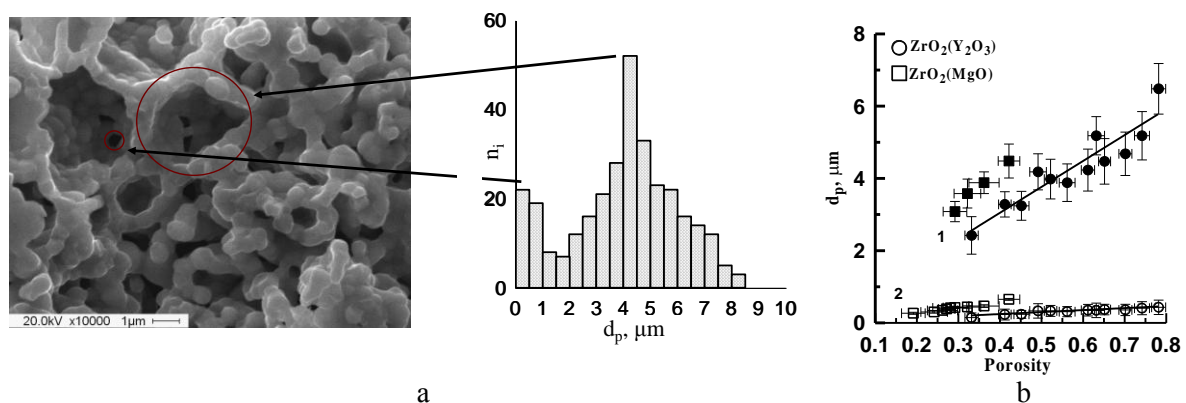


**Figure 2.** SEM-Picture of  $ZrO_2(Y_2O_3)$  ceramics structure, the characteristic pore size distribution of  $ZrO_2(MgO)$  ceramics with a porosity of  $\approx 40\%$  (a) and the dependence of the average pore size vs. porosity of  $ZrO_2$  ceramics (b). 1) - the average size of large pores spherical-like shape; 2) - the average size of interparticle pores.

From the data presented in Fig. 2 (b) dependences of interparticles pores and larger spherical pores from porosity in ceramics  $ZrO_2(MgO)$  and  $ZrO_2(Y_2O_3)$  it is seen that the increase in the volume of pores in the material from  $\approx 30$  to 80 % was achieved by reducing the sintering temperature of the samples and it was accompanied by an increase in the average size of large pores from 2 to 6 microns.

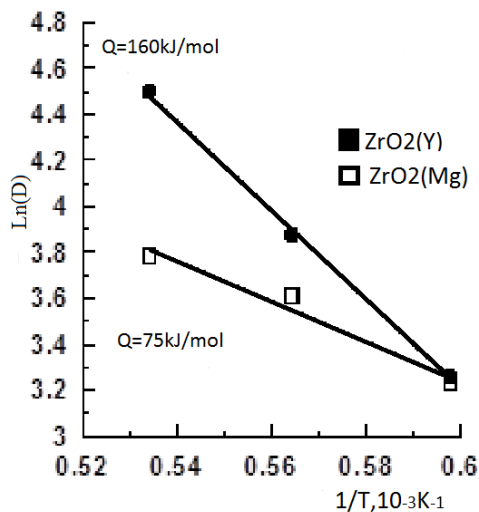


**Figure 3.** The activation energy calculated from dependence of the crystallites size vs sintering temperature of porous ceramics ZrO<sub>2</sub>

Changing the porosity of the material had practically no influence on the average size of interparticles pores, the average size of which was 0.5 microns. It can be assumed that the presence of large pores close to a spherical shape in the ceramics is due to the presence of hollow spherical particles in source powders, since their average size is commensurate with an average size of presented large pores in the sintered material.

In this study we have determined the activation energy of the crystallites growth for ZrO<sub>2</sub>(Y<sub>2</sub>O<sub>3</sub>) and ZrO<sub>2</sub>(MgO) ceramics, Fig.3. It was obtained according to re-plotting of crystallite sizes with increasing sintering temperature, fig.6. Activation energy for growth of crystallites of ZrO<sub>2</sub>(Y<sub>2</sub>O<sub>3</sub>) was 160 kJ/mol, for system ZrO<sub>2</sub>(MgO) – 75 kJ/mol, fig. 6, these values are well agree with literature data [13], suggest that the predominant mechanism in the sintering ZrO<sub>2</sub>(MgO) is the surface diffusion and for the system ZrO<sub>2</sub>(Y<sub>2</sub>O<sub>3</sub>) is a bulk diffusion.

### 3.3. Biocompatibility: cytotoxicity and osteogenic differentiation of MSCs

Cultured adipose tissue-derived MSCs used for a preliminary assessment of the biocompatibility of porous ceramic implants had the capacity to differentiate into adipogenic and osteogenic directions and had the following phenotype: CD73+ CD90+ CD105+ and CD34- CD45-. Combined staining of FDA/PI cells cultured on the surface or in the implants showed no cytotoxicity of porous ZrO<sub>2</sub> ceramics (Fig. 4). The results of evaluation of the viability of cells in suspension with use of Trypan blue staining before seeding and 24h after culturing on implants by staining with FDA/PI revealed similar values (suspension, Trypan blue – 96.42 ± 1.8% viable cells; implant, FDA/PI – 93.78 ± 2.15%). Microscopic observation showed that MSCs 24h after seeding adhered to the surface of the implant and generated intensive and uniform green FDA stain in the absence of red PI stain, which indicates a high metabolic activity of the cells and the integrity of their membrane. At the same time the cells had different spreading degree due to the rough surface of the implant through its physical structure (the presence of pores and composition of hollow particles of a spherical shape and a large number of units having no regular form). Cell viability after 7 days of culture with porous ZrO<sub>2</sub> ceramic implants was 92.56 ± 1.44%, which is comparable to cell viability before seeding and after 24h culturing with implants (difference not statistically significant). Moreover, after 7 days of MSC culturing on the surface of porous ZrO<sub>2</sub> ceramics, it should be noted the presence of cell clusters due to their proliferation. Thus, porous ZrO<sub>2</sub> ceramic implants do not have the acute and chronic cytotoxicity. Detection of alkaline phosphatase activity with use of BCIP/NBT substrate showed that cultured MSCs on the porous surface of ZrO<sub>2</sub> ceramic implant retain their ability for osteogenic differentiation (Fig. 5). Based on the results of the osteogenic differentiation of MSCs we can conclude that porous ZrO<sub>2</sub> ceramic implants possess osteoconductive properties.

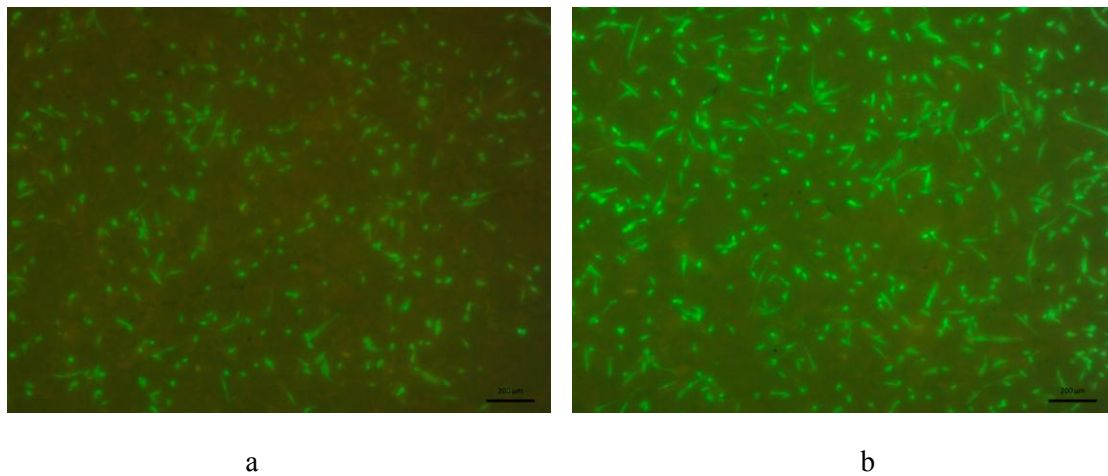


**Figure 4.** Viability assessment of MSCs cultured on the porous surface of the ZrO<sub>2</sub> ceramic implants for 24h (a) and for 7 days (b). Combined FDA/PI stain.

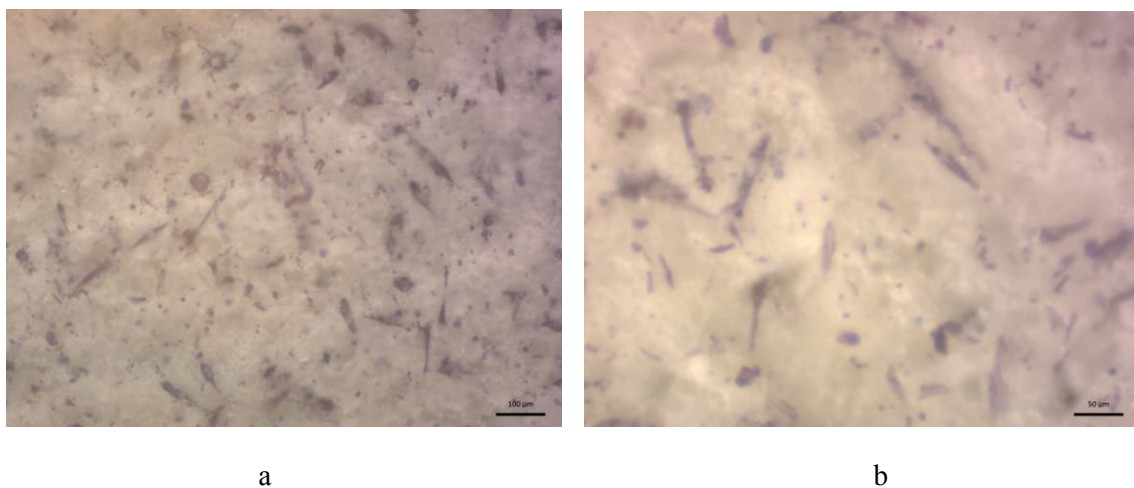


**Figure 5.** Detection of alkaline phosphatase activity after osteogenic differentiation of MSCs cultured on the porous ZrO<sub>2</sub> ceramic implants. BCIP/NBT stain.

#### 4. Conclusions

It was shown that the structure of ZrO<sub>2</sub>(Me<sub>x</sub>O<sub>y</sub>) ceramics, obtained from the powders consisting of hollow spherical particles with a porosity more 30 % is represented as a cellular carcass with a bimodal porosity, formed of a large pore close to a spherical shape and the pores that were not filled with the powder particles during the compaction.

It was found that in the range of sintering temperatures 0.56-0.63 ceramic ZrO<sub>2</sub>(MgO) activation energy of crystallite growth of 75 kJ/mol, which corresponds to the surface diffusion, and for ceramic ZrO<sub>2</sub>(Y<sub>2</sub>O<sub>3</sub>), 160 kJ/mole, which corresponds to the bulk diffusion.

It was also shown that the porous ZrO<sub>2</sub> ceramics had no acute or chronic cytotoxicity. At the same time, the porous ZrO<sub>2</sub> ceramics possess the osteoconductive properties: adhesion support, spreading, proliferation and osteogenic differentiation of MSCs.

### Acknowledgments

This work is partial financial supported by Tomsk State University Competitiveness Improvement Program and Grant No 14.607.21.0069-RFMEFI60714X0069 of Ministry of Sciences and Education of RF.

### References

- [1] L A Gomze and L N Gomze 2009 *Epitoanyag* **61** 38
- [2] L A Gomze, L N Gomze 2013 *IOP Conf. Ser.: Mater. Sci. Eng.* **47** 012033
- [3] S. Kulkov, V. Maslovskii and S. Buyakova 2002 *Technical Physics, The Russian Journal of Applied Physics* **47** (3) 320
- [4] S N Kulkov, S P Buyakova, L A Gomze 2014 *Epitoanyag* **66** 2
- [5] E S Kalatur, S P Buyakova, S N Kulkov, I Gotman, I Kocserha 2014 *Epitoanyag* **66** 31
- [6] E Kalatur, A Kozlova, S Buyakova and S Kulkov 2013 *IOP Conf. Ser.: Mater. Sci. Eng.* **47** 012004
- [7] J Will, R Melcher, C Treul, N Travitzky, U Kneser, E Polykandriotis, R Horch and P Greil 2008 *J Mater. Sci. Mater. Med.* **19** 2781
- [8] M Dominici, K Le Blanc, I Mueller, I Slaper-Cortenbach, F Marini, D Krause, R Deans, A Keating, D Prockop and E Horwitz 2006 *Cytotherapy* **8** 315
- [9] R I Freshney 2010 *Culture of animal cells: a manual of basic technique and specialized applications*, **6** ed. Wiley-Blackwell, New Jersey
- [10] S Johnston, V Nguyen and D Coder 2013 *Curr. Protoc. Cytom.* **64** 9.2.1
- [11] D Prockop, D Phinney and B Bunnell 2008 *Mesenchymal stem cells: methods and protocols*, Humana Press, Totowa, NJ
- [12] J D Jang, S J Kim, H M Yoon and D Ch Shin 2011 *Tissue Eng Regen. Med.* **8** 371
- [13] P Kofstad 1972 *Nonstoichiometry diffusion and electrical conductivity in binary metal oxides* / N.Y. Wiley 379 p